

# Cavity cooling a single charged nanoparticle.

J. Millen\*, P. Z. G. Fonseca, T. Mavrogordatos, T. S. Monteiro<sup>†</sup> & P. F. Barker<sup>‡</sup>

The development of laser cooling coupled with the ability to trap atoms and ions in electromagnetic fields, has revolutionised atomic and optical physics, leading to the development of atomic clocks, high-resolution spectroscopy and applications in quantum simulation and processing. However, complex systems, such as large molecules and nanoparticles, lack the simple internal resonances required for laser cooling. Here we report on a hybrid scheme that uses the external resonance of an optical cavity, combined with radio frequency (RF) fields, to trap and cool a single charged nanoparticle. An RF Paul trap allows confinement in vacuum, avoiding instabilities that arise from optical fields alone, and crucially actively participates in the cooling process. This system offers great promise for cooling and trapping a wide range of complex charged particles with applications in precision force sensing<sup>1</sup>, mass spectrometry, exploration of quantum mechanics at large mass scales<sup>2,3</sup> and the possibility of creating large quantum superpositions<sup>4</sup>.

Light is an exceptionally flexible and precise tool for controlling matter, from trapping single atoms<sup>5</sup> to the optical tweezing of organic cells<sup>6</sup>. Laser cooling of atoms has led to the production of the Bose-Einstein condensate<sup>7</sup> and confinement in optical lattices<sup>8</sup>, allowing the exploration of quantum physics. The control of nano- and micro-scale systems with light has enabled the study of mesoscopic dynamical and thermodynamical processes<sup>9–11</sup>. In recent years it has been possible to control the motion of nanoscale oscillators at the quantum level using light<sup>12,13</sup>, which is seen to be of fundamental importance for the construction of quantum networks<sup>14–16</sup>, and has enabled the generation of nonclassical states of light<sup>17</sup>.

The creation of long-lived macroscopic quantum states of nanomechanical oscillators is challenging due to strong coupling with the environment. A mechanical oscillator, such as a nanosphere, that is levitated in vacuum minimizes the coupling to the environment. The lack of clamping leads to extremely high mechanical quality factors<sup>18</sup> ( $Q \approx 10^{12}$ ) offering force sensing with exquisite sensitivity<sup>1</sup>. Active feedback cooling has achieved milli-Kelvin centre-of-mass temperatures<sup>19,20</sup>. In addition, the ability to change the properties of the oscillator by changing the levitating field, and even to rapidly turn off the levitation, offers the prospect of interferometry in the absence of any perturbations other than gravity<sup>21</sup>.

Cavity cooling<sup>22</sup> has been used to cool atoms<sup>23,24</sup> and atomic ions<sup>25</sup>, and it has been predicted that it could be used to cool larger particles to the centre-of-mass quantum ground-state<sup>18,26,27</sup>. The cooling of neutral nanoparticles transiting a cavity in vacuum<sup>28</sup>, and trapped at 1 mbar<sup>29</sup>

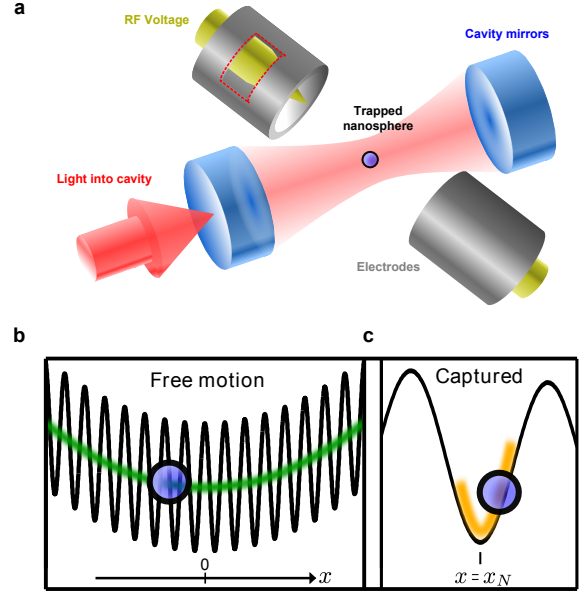


**Figure 1: Hybrid electro-optical trap used to levitate and cool a charged silica nanosphere in vacuum.** **a**, A schematic diagram of the hybrid trap, consisting of a Paul trap and standing wave optical cavity potential. **b**, The sphere is trapped by the Paul trap and driven across the standing wave formed by the light in the cavity, scattering light. **c**, When cooled, the sphere is trapped by the optical field and confined to one fringe of the standing wave.

has been demonstrated.

We present a new method for cavity cooling charged nanoparticles, utilizing both the optical field of a cavity and the electric field of a Paul trap. Crucially, the Paul trap drives the cavity cooling dynamics by introducing a cyclic displacement of the equilibrium point of the mechanical oscillations in the optical field. In addition the deep Paul trap potential avoids instabilities that have been observed in all-optical traps at low pressures<sup>11,30</sup>, and allows us to operate in vacuum.

A schematic diagram of the hybrid electro-optical trap which combines both a Paul trap and an optical cavity dipole trap is shown in fig. 1a.

The Paul trap potential for a nanosphere is approximated by

$$V(x, y, z, t) = \frac{1}{2} m \omega_T^2 (x^2 + y^2 - 2z^2) \cos(\omega_d t), \quad (1)$$

where  $m$  is the mass of the nanosphere and  $\omega_T^2 = \frac{2qV_0}{mr_0^2}$ , with  $q$  the charge on the nanosphere, and  $r_0$  a parameter setting the scale of the trap potential.

The optical cavity field creates a potential given by  $V_{\text{opt}}(x, y, z) = U_0 \cos^2 kx e^{-2(y^2+z^2)/w^2}$  where the depth of the optical potential  $U_0 = \hbar A |\alpha|^2$ ; here  $|\alpha|^2$  is the intra-cavity photon number and the coupling strength  $A =$

\* j.millen@ucl.ac.uk

† t.monteiro@ucl.ac.uk

‡ p.barker@ucl.ac.uk

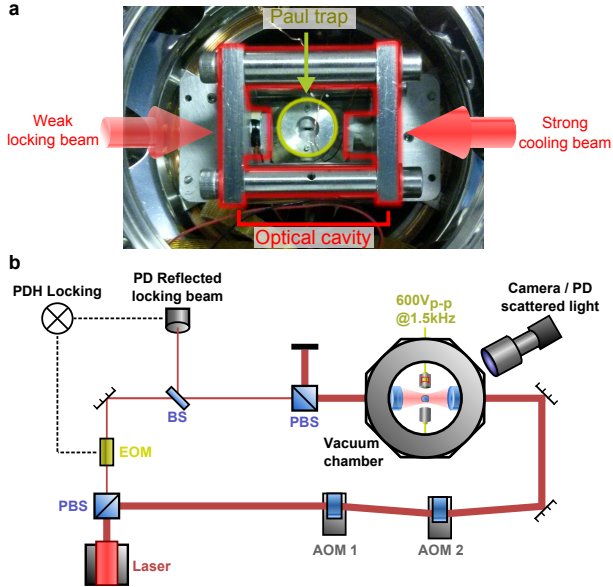


**Figure 2: Experimental setup for trapping and cooling nanospheres.** **a**, A photograph of the experiment. A Paul trap sits in the middle of an optical cavity. **b**, Optical layout for cooling. A weak beam resonant with the optical cavity is used to stabilize the cavity through Pound-Drever-Hall locking, and a beam at least fifty times more intense, which is used for trapping and cooling, can be detuned from the cavity resonance. The light which the nanosphere scatters as it moves through the optical cavity field is collected.

$\frac{3V_s}{2V_m} \frac{\epsilon_r - 1}{\epsilon_r + 2} \omega_1$  depends on the sphere volume  $V_s$ , the mode volume  $V_m = \pi w^2 L$  (with  $w$  the waist of the cavity field and  $L$  the length of the cavity) and the laser frequency  $\omega_1$ . The optical potential gives rise to a mechanical frequency  $\omega_M$ , which in the experiments presented in this paper is  $\omega_M \simeq 2\pi \times 18$  kHz.

We define two regimes of motion within the hybrid trap. Free motion refers to when the particle is driven across the optical standing wave potential by the Paul trap (fig. 1b), while captured motion corresponds to where the nanosphere is confined and oscillates within a single well of the standing wave (fig. 1c), where most of the cooling takes place.

Near turning points of the Paul trap motion (where the speed of the nanoparticle is a minimum) a small amount of damping can lead to the nanosphere losing enough energy to be captured by the optical potential within a well at  $x = x_N$  (fig. 1c). Optomechanical damping of the motion of the nanosphere occurs when the light is red detuned with respect to the cavity resonance. The damping occurs as the nanosphere oscillates across the optical potential well in the antinode of the light field. This motion modulates the effective cavity length and periodically brings the cavity closer to resonance, increasing the intracavity power and thus the optical potential. Due to the decay time of light in the cavity the intracavity build-up is delayed with respect to the motion, which causes damping<sup>26</sup>. In the absence of the Paul trap field, the nanosphere is cooled by the light towards the bottom of a local standing wave potential well (optical antinode). In this region, cooling is ineffective as the nanosphere's motion does not significantly modulate the cavity length. However, in our hybrid system, the additional force on the charged nanosphere by the Paul trap acts to periodically pull the particle away from the anti-node, leading to enhanced cooling. The oscillation within the optical potential is therefore asymmetric around the bottom of the

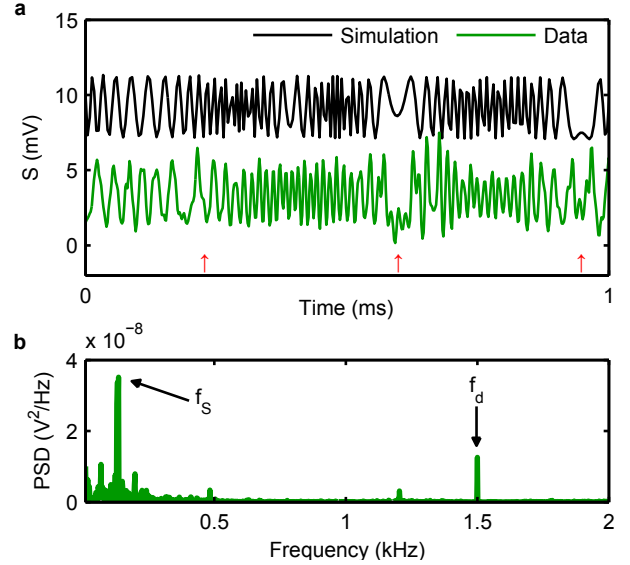


**Figure 3: Free motion of the nanosphere in the Paul trap.** **a**, The scattered signal  $S$  as the Paul trap drives the nanosphere across the optical standing wave, with a simulation showing the predicted dynamics. The turning points of the motion are marked. **b**, During free motion the power spectral density (PSD) of the nanosphere's motion shows the Paul trap secular frequency  $\omega_S = 2\pi \times f_S$  and micromotion  $\omega_d = 2\pi \times f_d$ . Measurement of  $f_S$  allows readout of the charge, in this case just a single charge  $q/e = 1$ .

potential well as illustrated in fig. 1c.

To explore the cooling and particle dynamics in the hybrid trap, we use a Paul trap formed by two rounded electrodes separated by 1 mm. This traps nanospheres of radius 209 nm which typically have 1-3 elementary charges. An RF voltage of  $V_0 \cos(\omega_d t)$ , where  $V_0$  is the amplitude of the time-varying signal ranges from 300–900 V and  $\omega_d = 2\pi \times 1500$  Hz is its frequency, is applied to the electrodes. The electrodes are enclosed by grounded cylindrical shields. The intracavity field of a medium finesse ( $\mathcal{F} \simeq 15,000$ ) optical cavity passes through the middle of the Paul trap. The hybrid trap was placed within a vacuum chamber as shown in fig. 2a. The nanospheres can be trapped at all pressures down to the limit of  $10^{-6}$  mbar in the current setup. The laser used to provide the trapping and cooling light is split into a strong and weak beam. The weak beam is used to lock the laser to the cavity via the Pound-Drever-Hall method, as illustrated in fig. 2b. The strong beam is used for cooling and trapping and can be arbitrarily shifted in frequency with respect to the cavity resonance.

To observe the dynamics and characterize the cooling of a single particle, we measure the scattered light  $S$  as the nanosphere passes through the standing wave field. This provides a measurement of particle position as a function of time. Free motion of the particle produces a rapid modulation as the particle moves through many antinodes of the standing wave cavity field, as shown in fig. 3a. During free motion, the trajectory of the nanoparticle is well parametrized by the Paul trap secular  $\omega_S \simeq \frac{\omega_T^2}{\sqrt{2}\omega_d}$  and micromotion frequency  $\omega_d$  (see fig. 3b), despite the addition of the optical field.

However, when a particle is captured and cooled it oscillates around a single antinode and the time averaged scattered light increases. A time series recorded for both free and captured motion is shown in fig. 4, for two detunings

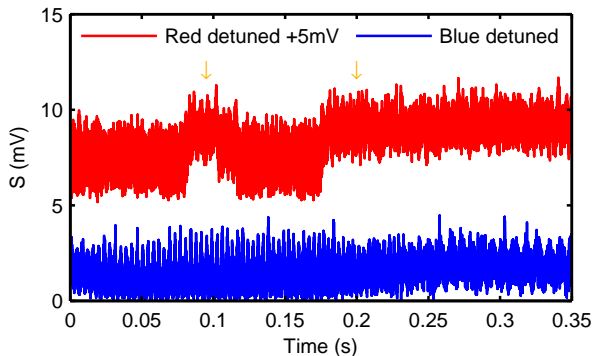


**Figure 4: Effect of detuning from the cavity resonance on the dynamics of the nanosphere.** Scattered light signal  $S$  from the nanosphere at a pressure of  $7.4 \times 10^{-3}$  mbar with  $\Delta \simeq \pm\kappa$ . When the light is red detuned from the cavity resonance (upper red trace, signal offset for clarity) there are periods of free motion in the Paul trap, and regions where the nanosphere is captured in the optical potential, where the particle can be cooled (marked at  $t \simeq 0.2$  s) or not (marked at  $t \simeq 0.1$  s) depending upon the location within the optical standing wave. The nanosphere is not captured by the optical potential when the light is blue detuned from the cavity resonance (lower blue trace) and is periodically heated out of the optical field.

from the cavity resonance. The red trace is taken for light that is red detuned and shows regions of increased intensity as the particle is captured in the standing wave potential. When captured the nanosphere is cooled, with greater cooling rates for captures far from the centre of the Paul trap. A similar trace for blue detuned light shows no capture (a constant mean scattered light intensity), as this detuning leads to heating of the particle motion.

Figure 5a shows the capture and initial cooling process. In this trace the initial rapid modulation is followed by a dip in intensity as the particle is trapped. The particle then starts to undergo a well defined motion in the optical well, showing period doubling as the Paul trap causes asymmetric oscillations about the optical antinode (as illustrated in fig. 1c). The period doubling is clear evidence that the Paul trap is modifying the dynamics within the optical potential, which is essential for efficient cooling. The average scattered light intensity increases as the nanosphere is cooled towards the optical antinode.

To quantify the optomechanical cooling we consider the motion of the nanosphere within one well of the optical potential  $x'(t) = x(t) - x_N$ . Within the optical potential a mechanical frequency  $\omega_M$  can be defined, which depends upon  $U_0$  as well as which well  $N$  of the standing wave the particle is confined to (see supplementary material for full details). Since  $\omega_M \gg \omega_S, \omega_d$  the motions due to the optical and Paul trap potentials are adiabatically separable; as  $t \rightarrow \infty$ , we approximate the motion along the optical axis by:

$$x'(t) \sim X_d \cos(\omega_d t) + X_M^\infty \cos(\omega_M t). \quad (2)$$

The drive amplitude  $X_d \approx \frac{\omega_d^2}{\omega_M^2} x_N$  is largely undamped.  $X_M^\infty$  is the steady-state amplitude of the mechanical motion; initially,  $X_M(t)$  decays as  $\sim e^{-\Gamma_{\text{opt}} t}$  but tends to a steady state value determined by noise heating processes. By analyzing the Fourier spectrum of  $S$  due to  $x'(t)$  one finds, to leading order, frequencies at  $\omega_M \pm \omega_d$  with amplitude  $A_1$  and a single peak at  $2\omega_M$  with an amplitude  $A_2$  (see supplementary material). The amplitudes of the Fourier peaks  $A_{1,2}$  are related to the amplitude of the motion of the nanosphere

through  $\frac{A_2}{A_1} \simeq \frac{J_0(2kX_d)J_2(2kX_M^\infty)}{J_1(2kX_d)J_1(2kX_M^\infty)}$  where  $J_n$  are Bessel functions of order  $n$  and  $\frac{A_2}{A_1} \rightarrow \frac{X_M^\infty}{X_d}$  for small amplitude oscillations. Hence, by analyzing the Fourier spectrum the cooling rate of the nanoparticle's motion can be measured.

In fig. 5b, the Fourier spectrum of captured nanosphere motion is shown. At a pressure of  $7.4 \times 10^{-3}$  mbar (grey line) the damping due to the background gas  $\Gamma_M \sim \Gamma_{\text{opt}}$ , hence no cooling is evident and  $A_2 > A_1$ . At a pressure an order of magnitude lower, where  $\Gamma_{\text{opt}} \gg \Gamma_M$  (orange line), both the capture and subsequent cooling are dominated by optomechanical damping and there is a significant reduction in the size of  $A_2$ . The width of peaks is due to the excursion of the nanosphere into the anharmonic regions of the optical potential.

We can also analyze the cooling by calculating the optomechanical damping rates directly. For small oscillations, the cooling of a levitated particle may be obtained from the well-known optomechanical quantum Hamiltonian:

$$\frac{\hat{H}_{\text{Lin}}}{\hbar} = -\Delta \hat{a}^\dagger \hat{a} + \frac{\omega_M}{2} (\hat{x}^2 + \hat{p}^2) + g(\hat{a} + \hat{a}^\dagger) \hat{x} \quad (3)$$

where  $\hat{x}$  is a small fluctuation (in units of  $X_{\text{ZPF}} = \sqrt{\hbar/2m\omega_M}$ ) about an equilibrium point  $x_0$  and  $\hat{a}$  is a fluctuation of optical field about the mean value  $\alpha$ . Whether in the quantum regime or not, the corresponding damping  $\Gamma_{\text{opt}}$  is then given by  $\Gamma_{\text{opt}} = g^2 \kappa [\mathcal{S}(\omega_M) - \mathcal{S}(-\omega_M)]$  where  $\mathcal{S}(\omega) = \left[ [\Delta - \omega]^2 + \frac{\kappa^2}{4} \right]^{-1}$ . Simulations with the full 3D nonlinear dynamics of the hybrid trap shows that the above expressions are accurate provided one allows for the slow excursion in the equilibrium point, since  $x_0 \equiv x_0(t) \simeq X_d \cos \omega_d t$  and the equilibrium point can be far from the antinode ( $0 \leq kX_d \lesssim \pi/2$ ). This consideration leads to an effective optomechanical coupling (see supplementary information):

$$g^2 = \frac{\hbar k^2 A^2 |\alpha|^2}{2m\omega_M} (1 - J_0(4kX_d)). \quad (4)$$

Using the experimental parameters for the data in fig. 5a ( $\mathcal{F} \simeq 15000$ ,  $\Delta = 2\pi \times 288$  kHz, intracavity power  $P = 14$  W,  $\omega_S = 2\pi \times 100$  Hz) we find  $\Gamma_{\text{opt}} \approx 20 - 30$  Hz, where the capture is at well position  $N = kx_N/\pi \simeq 600 - 700$ . The expected equilibrium temperature  $T_{\text{eq}} \simeq \frac{\Gamma_M}{\Gamma_{\text{opt}}} T_B$ , where here  $T_B = 300$  K, and  $\Gamma_M \simeq 1$  Hz at  $4.6 \times 10^{-4}$  mbar pressure. This means that the motion of the nanosphere is cooled to  $\sim 10$  K, which represents a factor of  $\sim 100$  reduction in energy from the well depth  $U_0$ . This reduction in energy is consistent with the Fourier analysis of the peaks in fig. 5b.

The nanospheres are confined within an optical well for a time of order 0.1-0.2s, far longer than the time needed to attain a steady state temperature (of order 10 ms). After this time they escape the optical potential since both the optomechanical coupling  $g$  and the optical potential  $U_0$  are very weak, and noise on the light field is sufficient to kick the nanospheres out of the well, a situation we have confirmed with simulations. Once the spheres are lost from the optical well they are recaptured by the Paul trap and returned to the cooling cycle. To solve the problem of loss from the optical potential a higher finesse optical cavity can be used, with a smaller mode volume  $V_m$ , since  $g^2 \propto V_m^{-2}$  and we can operate at the sideband-resolved regime  $-\Delta \simeq \omega_M \gtrsim \kappa/2$  which yields maximum cooling, and size of the optical potential  $U_0 \propto V_m^{-1}$  is enhanced. For example, for a cavity

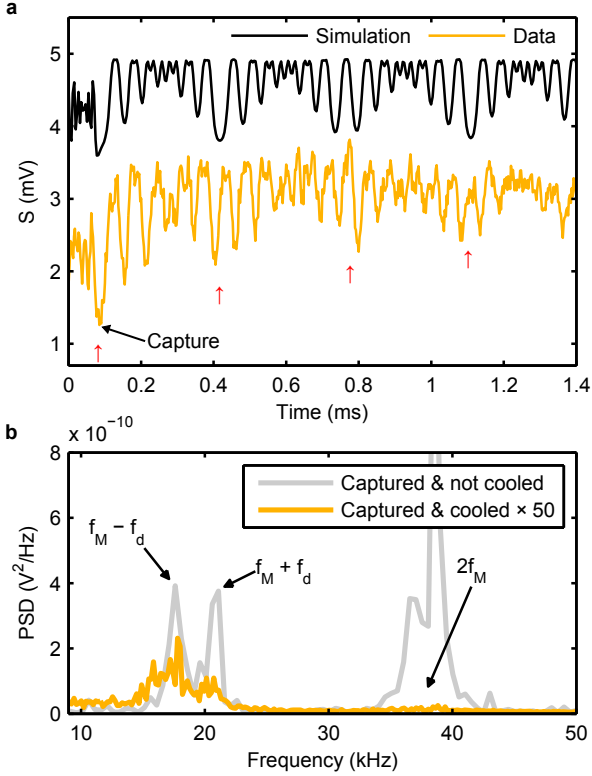


**Figure 5: Capture and optomechanical cooling of the nanosphere.** **a**, The scattered signal  $S$  once the nanosphere has been captured, at a pressure of  $4.6 \times 10^{-4}$  mbar, and a simulation of the process. The mechanical motion is cooled, and the motion due to the Paul trap is still present (marked by arrows). **b**, The PSD of the nanosphere’s motion while captured by the optical field. At a low pressure of  $4.6 \times 10^{-4}$  mbar (orange line) the split mechanical frequency  $f_M \pm f_d$  is visible, but the doubled frequency  $2f_M$  is heavily suppressed, indicating cooling. At a higher pressure of  $7.4 \times 10^{-3}$  mbar (grey line) mechanical damping from the background gas dominates and the nanoparticle is not cooled, as shown by the unsuppressed peak at  $2f_M$ .

with  $\mathcal{F} = 100,000$  and  $w = 60 \mu\text{m}$  cooling rates of  $\sim 10$  kHz are possible.

We have reached low temperatures with very low cooling rates of 30 Hz, and the introduction of a higher finesse optical cavity would greatly lower our final temperature. So far we have only discussed cooling in the  $x$  direction, along the optical axis. Our simulations show that cooling in the  $y$  and  $z$  directions can be achieved with the addition of a small angle between the coordinate systems of the optical and Paul trap fields.

In conclusion, we present a hybrid optical and quadrupole electric trap for both confining and optomechanically cooling charged levitated dielectric objects in high vacuum. Since the levitation is not by an optical field alone, light intensities that have been shown to melt silica nanospheres<sup>11</sup> do not have to be used. The system we present in this paper is very suitable for cooling nanoscale objects to the quantum level, in principle the only required modification is a higher finesse optical cavity. This work opens the way for the exploration of fundamental questions in quantum physics, and the development of macroscopic quantum technologies. Since Paul traps are used widely for the characterisation of nanoparticles, our work introduces a powerful new tool for their manipulation and the damping of their motion.

## Acknowledgements

We acknowledge support from the UK’s Engineering and Physical Science Research Council grant EP/H050434/1.

## Methods

Silica nanospheres of radius 209 nm (Corpuscular inc.), were sonicated in methanol for several hours to prevent clumping. The solution was dropped onto a ceramic piezoelectric speaker and allowed to dry. Nanospheres were launched into the trap from the speaker through a narrow aperture into the Paul trap, which is loaded at a pressure of  $2 \times 10^{-1}$  mbar. During loading the cavity mirrors are covered by a shield to protect them from the nanoparticles. However, the finesse of the cavity varied between  $\mathcal{F} = 10, 500 - 15,000$  over the course of the experiments due to contamination of the cavity mirrors by nanoparticles. The charge of the nanospheres could be ascertained from the Paul trap secular frequency  $\omega_S$ .

The Paul trap is mounted on a remotely-controllable, vacuum compatible,  $x - y - z$  translation stage which was used to align the trapped particle with the optical axis of the cavity. The cavity has a length of 3.7 cm a beam waist of  $140 \mu\text{m}$ .

# SUPPLEMENTARY INFORMATION

## I Dynamics in a Paul trap

The dynamics and stability properties of quadrupole ion traps have been extensively studied, given their importance for scientific research as well as applications such as ion mass spectrometry see (see<sup>32</sup> for a review), so here we simply outline some key features. A general Paul trap combines a DC static field with an AC component, oscillating with a drive frequency  $\omega_d$ . The corresponding potential is  $V_{\text{ion}}(x, y, z, \omega t) = V^{\text{AC}}(x, y, z, \omega t) + V^{\text{DC}}(x, y, z)$  with oscillating component:

$$V^{\text{AC}}(x, y, z, t) = \phi_0^{\text{AC}} (\beta_x x^2 + \beta_y y^2 + \beta_z z^2) \cos(\omega_d t), \quad (5)$$

and a DC field of a similar form:

$$V^{\text{DC}}(x, y, z) = -\phi_0^{\text{DC}} (\beta_x x^2 + \beta_y y^2 + \beta_z z^2), \quad (6)$$

where  $\phi_0^{\text{AC(DC)}} = QV_0(U_0)/r_0^2$ . Here,  $Q$  is the charge of the particle,  $V_0(U_0)$  is the applied AC(DC) voltage and the parameter  $r_0$  sets the scale of the Paul trap potential. For a 3D quadrupolar trap,  $\beta_x = \beta_y = 1$  while  $\beta_z = -2$ , constraints imposed by the requirement that the potential field obey Laplace’s equation. The resulting motion is separable; taking  $\mathbf{u} \equiv x, y, z$ , the force  $F_{\mathbf{u}} = -\partial V/\partial \mathbf{u}$  yields three equations of motion, one for each degree of freedom:

$$m\ddot{\mathbf{u}} = \frac{m\omega_d^2}{4} [a_{\mathbf{u}} - 2q_{\mathbf{u}} \cos(\omega_d t)]\mathbf{u}, \quad (7)$$

where the DC and AC stability parameters are respectively  $a_{x,y} = QU_0/(m\omega_d^2 r_0^2)$  and  $q_{x,y} = 4QV_0/(m\omega_d^2 r_0^2)$ , while

$a_z = -a_x$  and  $q_z = -2q_x$ . Eq.7 represents three equations in Mathieu form; these have been shown to be stable for specific ranges of  $a_u, q_u$ . In our experiment, we consider a Paul trap with zero applied DC voltage ( $U_0, a_u = 0$ ). In this case, the ion trap motion becomes unstable for  $q_u \gtrsim 0.91$ . Conversely, for small enough  $q_u \lesssim 0.2$ , the motion is not only stable but may also be adiabatically separated into a fast micromotion and a slower secular motion; the corresponding trajectories are given by:

$$u(t) \simeq u_0 \cos(\omega_S t) - u_0 \frac{q_u}{2} \cos(\omega_S t) \cos(\omega_d t), \quad (8)$$

where  $\omega_S^{(u)} \simeq \frac{\omega_d}{2} \sqrt{a_u + \frac{q_u^2}{2}}$  is the secular frequency and  $u_0$  an initial amplitude. In the main text we set  $\omega_S^{(x)} = \omega_S^{(y)} \equiv \omega_S$  noting that the equality signs strictly apply only to a perfectly quadrupolar trap and in the absence of perturbations arising from the cavity field (see below). We have redefined the ion trap potential in terms of a characteristic ion trap frequency  $\omega_T^2 = 2QV_0/(mr_0^2)$  which is typically of the same order as  $\omega_S$ . In the separable regime,  $\omega_T^2 \simeq \sqrt{2}\omega_d\omega_S$ .

## II Equations of motion in the hybrid trap

The combined dynamics of the hybrid cavity and Paul trap potentials requires the solution of coupled equations of motion for the mechanical degrees of freedom  $\hat{x}, \hat{y}, \hat{z}$  as well as the cavity light mode  $\hat{a}$ . The equations of motion are obtained here from the total Hamiltonian of the hybrid trap. In a frame rotating at the laser frequency  $\omega_l$ , the corresponding quantum Hamiltonian may be written:

$$\hat{H} = \frac{\hat{P}^2}{2m} - \hbar\Delta\hat{a}^\dagger\hat{a} + \hbar\mathcal{E}(\hat{a}^\dagger + \hat{a}) - V_{\text{opt}}(\hat{x}, \hat{y}, \hat{z}) + V^{\text{AC}}(\hat{x}, \hat{y}, \hat{z}, t). \quad (9)$$

The first term is the total kinetic energy operator of the nanoparticle;  $\Delta = \omega_l - \omega_c$  represents the detuning between the laser frequency and the resonant frequency of the cavity  $\omega_c$ . If  $\omega_l < \omega_c$ , the cavity is red-detuned.  $\mathcal{E}$  represents the driving amplitude of the cavity and is related to the input power  $P_{\text{in}}$  (for a critically coupled cavity) by  $\mathcal{E}^2 = \frac{\kappa}{2} \cdot \frac{P_{\text{in}}}{2\hbar\omega_l}$ . In the experimental regimes under consideration it is reasonable to assume semiclassical behaviour and replace the operators by scalar complex amplitudes  $\hat{a}(t) \rightarrow \langle \hat{a}(t) \rangle \equiv a(t)$ ; we write the optical potential as follows:

$$V_{\text{opt}}(x, y, z) = \hbar A |a(t)|^2 \cos^2(kx) \mathcal{F}(y, z) \quad (10)$$

where the transverse envelope of the light beam is  $\mathcal{F}(y, z) = \exp[-2(y^2 + z^2)/w^2]$ . The Paul trap potential is  $V^{\text{AC}} = \frac{1}{2} m \omega_T^2 (x^2 + y^2 - 2z^2) \cos(\omega_d t)$ . Hence, we obtain equations of motion for the axial degree of freedom (along the optical axis):

$$\ddot{x} = -\frac{\hbar k A}{m} |a(t)|^2 \sin(2kx) \mathcal{F}(y, z) - \Gamma_M \dot{x} - \omega_T^2 x \cos(\omega_d t), \quad (11)$$

the transverse motions:

$$\begin{aligned} \ddot{y} &= -\frac{4y}{w^2} \frac{\hbar A}{m} |a(t)|^2 \cos^2(kx) \mathcal{F}(y, z) - \Gamma_M \dot{y} - \omega_T^2 y \cos(\omega_d t), \\ \ddot{z} &= -\frac{4z}{w^2} \frac{\hbar A}{m} |a(t)|^2 \cos^2(kx) \mathcal{F}(y, z) - \Gamma_M \dot{z} + 2\omega_T^2 z \cos(\omega_d t). \end{aligned} \quad (12)$$

and for the cavity field:

$$\dot{a} = i\Delta a - i\mathcal{E} + iAa \cos^2(kx) \mathcal{F}(y, z) - \frac{\kappa}{2} a. \quad (13)$$

where we have added terms to account for the mechanical damping (of rate  $\Gamma_M$ ) due to collisions with residual background gas and optical decay terms (of rate  $\kappa/2$ ) due to losses at the cavity mirrors. The resulting set of coupled nonlinear equations were solved to simulate the free motion, capture process as well as trapping and cooling. In the trapped and cooling regimes however, the optical potential is dominant and oscillations are small. Thus we can analyse the motion by linearising about equilibrium values.

## III Optically trapped particle

For a particle which has been trapped at the  $N$ -th optical well, it is most convenient to switch to a local coordinate frame with the origin at the antinode,  $x = x_N$ , of the trapping well; hence, we transform the axial coordinates to  $x' = x - x_N$  and obtain for the axial motion:

$$\ddot{x}' = -\frac{\hbar k A}{m} |a(t)|^2 \sin(2kx') \mathcal{F}(y, z) - \Gamma_M \dot{x}' - \omega_T^2 (x' + x_N) \cos(\omega_d t). \quad (14)$$

For optically levitated particles, consideration of small oscillations about a point  $x' = x_0$  determines a mechanical frequency  $\omega_M$  where typically  $\omega_M \gg \omega_d, \omega_S$ . Thus we assume that the fast oscillations near the antinode are adiabatically separable from the slower timescales associated with the quadrupole trap. We write  $x'(t) = x_0(t) + x(t)$ , where we assume that the amplitude of the (fast varying)  $x(t)$  is small with respect to the slower oscillations  $x_0(t)$ . In the first instance, we assume a quasistatic  $x_0(t) \simeq x_0$  and obtain for the axial motion:

$$\ddot{x}_0 + \ddot{x} = -\frac{\hbar k A}{m} |a(t)|^2 \cos(2kx_0) [\sin(2kx) + \tan(2kx_0) \cos(2kx)] - \omega_T^2 x_N \cos(\omega_d t) \quad (15)$$

where we neglect damping due to the presence of the gas (see end of the section) and assume that the particle is caught in a well such that  $x_N \gg x'$ .

Similarly, if we assume temporal fluctuations in the cavity field are small, we can also transform to shifted values for the field amplitudes hence  $a(t) \rightarrow \bar{\alpha} + a(t)$  where  $\bar{\alpha}^2$  represents the mean cavity photon number and  $a(t)$  are now small fluctuations about the mean.

Keeping only zero-th order terms in equation (15) and assuming that  $|\dot{x}_0| \ll |\ddot{x}|$  we obtain:

$$\omega_M^2 \tan(2kx_0) \approx -2kx_N \omega_T^2 \cos(\omega_d t), \quad (16)$$

where we write  $\omega_M^2 \simeq (2\hbar k^2 A \mathcal{F}(y, z) |\bar{\alpha}|^2 / m) \cos(2kx_0)$  (and we show below that  $\omega_M$  is in fact the mechanical frequency of our system).

Recalling that  $x_0(t)$  is time-dependent and is oscillating (albeit slowly), the above can be recast in the form:

$$\sin(2kx_0(t)) \approx -\frac{\omega_T^2}{\omega_M^2} (2kx_N) \cos(\omega_d t). \quad (17)$$

Hence if  $x_0$  remains small for all  $t$  then  $x_0(t) \approx -\frac{\omega_T^2}{\omega_M^2} x_N \cos(\omega_d t)$ ; however, we do not need to assume this: the excursion in  $x_0$  can in fact span a significant

fraction of the well; in that case, the mechanical frequency  $\omega_M(t)$  varies within the range  $\omega_M[1 - \sqrt{\cos(2kX_d)}]$ , which is approximately 15% of  $\omega_M$  for an oscillation about a distance of  $\lambda/4$  from the bottom of the optical potential well. This variability in  $\omega_M$  leads to broadening of the peaks in Fig.(3) of the main text. For simplicity, we assume in the analysis below (but not in our numerical simulations) that the transverse excursions are small and thus  $\mathcal{F}(y, z) \simeq 1$ . However, in fact these excursions remain detectable and even for the trapped particle, the scattered light detects oscillations at one or both transverse secular frequencies  $\omega_S^{(y,z)} = [\omega_d/(2\sqrt{2})]q_{y,z}$ . The transverse oscillations are important for sensing the full 3-dimensional particle trajectories; as they are only weakly affected by the optical potential they provide a reliable measurement of the nanoparticle's charge,  $Q$ . If the transverse motions become significant, they lead to further variability in  $\omega_M$  and more importantly, to escape from the optical well.

The zero-th order terms in the equation for the optical field yield a value for the mean intracavity fields:

$$|\bar{\alpha}|^2 = \frac{\mathcal{E}^2}{\kappa^2/4 + \Delta^2} \quad (18)$$

where  $\Delta$  includes a small correction from the optical field<sup>31</sup> which is neglected here as the coupling to the optical field  $A$  is not very strong.

The optomechanical coupling which leads to optical damping is contained in the first order equations for  $x(t)$ :

$$\ddot{x} = -\omega_M^2 x - \frac{\hbar k A}{m} \bar{\alpha}(a + a^*) \sin(2kx_0) - \Gamma_M \dot{x} \quad (19)$$

where, without loss of generality, we have assumed that  $\bar{\alpha}$  is real. (eg in the Hamiltonian, by means of the transformation  $\bar{\alpha} \rightarrow \bar{\alpha}e^{-i\theta}$  and  $\hat{a} \rightarrow \hat{a}e^{i\theta}$  we can restrict ourselves to real  $\bar{\alpha}$ ).

For  $a(t)$  we obtain:

$$\dot{a} = i\Delta a - ikA\bar{\alpha}x \sin(2kx_0) - \frac{\kappa}{2}a. \quad (20)$$

For red-detuning ( $\Delta < 0$ ) the  $x(t)$  motion is damped such that  $x(t) \simeq X_M e^{-\Gamma_{\text{opt}} t} \cos(\omega_M t)$  where  $X_M$  is the initial amplitude for mechanical oscillations (soon after capture by an optical well). Thus the mechanical motion cools until a steady state is achieved whereby heating rates due to residual gas collisions or technical noise equals the cooling rate (see<sup>31</sup> for a study in levitated systems) and hence  $X_M e^{-\Gamma_{\text{opt}} t} \rightarrow X_M^\infty$  where  $X_M^\infty$  is a steady state amplitude which may fluctuate in time due to background noise; in effect  $\langle (X_M^\infty)^2 \rangle$  represents a good estimate of the variance of the mechanical motion and hence provides an estimate of the effective temperature of our system.

Finally, we combine the mechanical oscillations with the slower excursion in the equilibrium point to model the axial motion of the captured nanoparticle:

$$x'(t) \approx X_d \cos(\omega_d t) + X_M^\infty \cos(\omega_M t). \quad (21)$$

#### IV Analysis of the experiment

The intensity of the scattered light field from a point particle is proportional to the term  $S = \cos^2(kx'(t))\mathcal{F}(y, z)$ . The

experiment uses spheres of radius  $R = 200$  nm. For the transverse motion, the sphere dimensions are small relative to the beam waist  $w = 145 \mu\text{m}$  so a point particle approximation is quite reasonable. However, this is not the case in the axial direction given the standing wave potential for  $\lambda/2 = 532$  nm. A previous study of the effect of the particle size on the optical coupling parameter  $A$ <sup>31</sup> showed that the behaviour  $R = 200$  nm remains qualitatively similar to an point dipole particle. Nevertheless, for accuracy, here we convolve the scattering function with a sphere of finite size in our simulations and calculate for our scattering function:

$$S(t) = \bar{S}(t)\mathcal{F}(y(t), z(t)), \quad (22)$$

where:

$$\begin{aligned} \bar{S}(t) &= \frac{1}{2} - \frac{3}{16(kR)^3} \cos(2kx'(t))[2kR \cos(2kR) - \sin(2kR)] \\ &= \frac{1}{2} + C(kR) \cos(2kx'(t)). \end{aligned} \quad (23)$$

The Fourier transform of the scattered field, yielding the frequency spectrum of scattered radiation, allows us to extract the characteristic frequencies of the motions.  $\mathcal{F}(y(t), z(t))$  is modulated at the lowest frequencies (of order 100 Hz) by the transverse secular frequencies  $\omega_S^{(y)}$  and  $\omega_S^{(z)}$ ; Fourier transforms of traces of order several seconds show these clearly.

We focus now on Fourier transforms of the trapped regions, dominated by the mechanical and drive frequencies. The scattered signal, in frequency space may be calculated using Eqs.21 and 23:

$$\bar{\mathbf{S}}(\omega) = C(kR) \sum_{(m,n)} (-1)^l J_m(2kX_M^\infty) J_n(2kX_d) \delta[\omega - (m\omega_M + n\omega_d)], \quad (24)$$

where  $m + n = 2l$ ,  $l \in Z$ , while peaks with  $m + n = 2l + 1$  are absent from the spectrum. The relative amplitude of the peaks  $(m, n)$  and  $(m', n')$  in the spectrum is:

$$\mathcal{A}_{\text{rel}} = \frac{J_{m'}(2kX_M^\infty) J_{n'}(2kX_d)}{J_m(2kX_M^\infty) J_n(2kX_d)}. \quad (25)$$

If  $X_M^\infty \ll X_d \lesssim (1/k)$  then  $\mathcal{A}_{\text{rel}} \sim \frac{\Gamma(m+1)}{\Gamma(m'+1)} (kX_M^\infty)^{m'-m}$ , leading to an exponential reduction of higher order peaks (here  $\Gamma$  is the Gamma function).

Inspection of Eq.24 shows that the dominant terms in the spectrum involving the mechanical frequency are:

$$C(kR)^{-1} \bar{\mathbf{S}}(\omega) \sim \bar{\mathbf{S}}_1^+(\omega) + \bar{\mathbf{S}}_1^-(\omega) + \bar{\mathbf{S}}_2(\omega) \quad (26)$$

where:

$$\bar{\mathbf{S}}_1^\pm(\omega) \simeq \mp J_1(2kX_M^\infty) J_{\pm 1}(2kX_d) \delta(\omega - \omega_M \pm \omega_d) \quad (27)$$

and

$$\bar{\mathbf{S}}_2(\omega) = -J_0(2kX_d) J_2(2kX_M^\infty) \delta(\omega - 2\omega_M). \quad (28)$$

The first terms  $\bar{\mathbf{S}}_1^\pm(\omega)$  predicts a pair of peaks of similar amplitude centred at frequencies  $\omega_M \pm \omega_d$ . The second term  $\bar{\mathbf{S}}_2(\omega)$  produces a peak at the second harmonic (i.e. at double the mechanical frequency). We find that both these features are a common feature of Fourier transforms in the trapped regime although the experimental peaks are broadened due to the spread in  $\omega_M$  as well as other thermal broadening effects.

An important point is that the relative amplitudes of these peaks provide a means to estimate the steady state amplitudes  $X_M^\infty$  and thus enable an estimate the equilibrium temperature of the nanosphere. In particular, if there is strong cooling:

$$\left| \frac{J_0(2kX_d)J_2(2kX_M^\infty)}{J_{\pm 1}(2kX_d)J_1(2kX_M^\infty)} \right| \sim \frac{X_M^\infty}{X_d} \rightarrow 0, \quad (29)$$

resulting in the suppression of the second harmonic ( $2\omega_M$ ) peak in the spectrum. Thus we expect that those traces for which the second peak is weak or nearly absent correspond to the strongest cooling. In this case, we estimate the reduction in temperature from  $\frac{T_{\text{eq}}}{T_{\text{int}}} \sim \left[ \frac{X_M^\infty}{X_M(t=0)} \right]^2$  where  $T_{\text{int}}$  corresponds to an initial temperature which we can choose to define either as the height of the optical well or of a bath at  $T = 300$  K while  $T_{\text{eq}}$  is our final equilibrium temperature.

## V Optomechanical cooling rates $\Gamma_{\text{opt}}$

In the regime of separable mechanical and drive motion (where Eq.21 is a good approximation), the optomechanical damping may be calculated by standard methods (e.g. Linear Response theory as applied to Eqs.19 and 20).

Alternatively, we note that Eqs.19 and 20 are the equations of motion corresponding (in the semiclassical limit) to a well-studied effective Hamiltonian which describes typical optomechanical systems:

$$\frac{\hat{H}_{\text{lin}}}{\hbar} = -\Delta \hat{a}^\dagger \hat{a} + \omega_M \hat{b}^\dagger \hat{b} + g(\hat{a} + \hat{a}^\dagger)(\hat{b} + \hat{b}^\dagger)/\sqrt{2} \quad (30)$$

where the coordinates have been rescaled  $\hat{x} \rightarrow \sqrt{2}X_{\text{ZPF}}\hat{x}$ , while  $\hat{p} \rightarrow \sqrt{\hbar m\omega_M}\hat{p}$  and  $\hat{x} = (\hat{b} + \hat{b}^\dagger)/\sqrt{2}$ . Here,  $X_{\text{ZPF}} = \sqrt{\hbar/2m\omega_M}$  gives the scale of the oscillator ground state (zero-point fluctuations).

The dynamics corresponding to Eq.30 are extensively investigated and the corresponding the optical damping  $\Gamma_{\text{opt}}$  has been shown to be given by:

$$\Gamma_{\text{opt}} = g^2 \kappa [S(\omega_M) - S(-\omega_M)] \quad (31)$$

$$\text{where } S(\omega) = \left[ (\Delta - \omega)^2 + \frac{\kappa^2}{4} \right]^{-1}.$$

For the case of the levitated system investigated here, Eqs.19 and 20 are fully equivalent to the Hamiltonian Eq.30 provided we set for the instantaneous optomechanical coupling:

$$g^2(t) = \frac{\hbar k^2 A^2 \bar{\alpha}^2}{m\omega_M} \sin^2(2kx_0(t)) \quad (32)$$

with  $\omega_M^2 \simeq (2\hbar k^2 A \bar{\alpha}^2/m) \cos(2kx_0) \approx 2\hbar k^2 A \bar{\alpha}^2/m$  since  $\omega_M$  is less sensitive to the excursion in  $x_0$ .

$$\text{Averaging over the period of the micromotion } T_d = \frac{2\pi}{\omega_d}:$$

$$\frac{1}{T_d} \int_0^{T_d} \cos(4kX_d \cos(\omega_d t)) dt = \frac{1}{2\pi} \int_0^{2\pi} \cos(4kX_d \cos(u)) du = J_0(4kX_d) \quad (33)$$

we obtain:

$$\bar{g}^2 = \frac{\hbar k^2 A^2 \bar{\alpha}^2}{2m\omega_M} [1 - J_0(4kX_d)]. \quad (34)$$

The cooling rates are thus obtained by setting  $\bar{g} \equiv g$  in Eq.31.

## References

- 1 Geraci, A. A., Papp, S. B. and Kitching, J. Short-Range Force Detection Using Optically Cooled Levitated Microspheres. *Phys. Rev. Lett.* **105**, 101101 (2010)
- 2 Diósi, L. A universal master equation for the gravitational violation of quantum mechanics. *Phys. Lett. A* **120**, 377 (1987)
- 3 Penrose, R. On gravity's role in quantum state reduction. *Gen. Relativ. Gravit.* **28**, 581 (1996)
- 4 Arndt, M. and Hornberger, K. Testing the limits of quantum mechanical superpositions. *Nature Phys.* **10**, 271 (2014)
- 5 Schlosser, N., Reymond, G., Protsenko, I., and Grangier, P. Sub-poissonian loading of single atoms in a microscopic dipole trap. *Nature* **411**, 1024 (2001)
- 6 Ashkin, A., Dziedzic, J. M., and Yamane, T. Optical trapping and manipulation of single cells using infrared laser beams. *Nature* **330**, 769 (1987)
- 7 Leggett, A. J. Bose-Einstein condensation in the alkali gases: Some fundamental concepts. *Rev. Mod. Phys.* **73**, 307 (2001)
- 8 Bloch, I. Ultracold quantum gases in optical lattices. *Nature Phys.* **1**, 23 (2005)
- 9 Li, T., Kheifets, S., Medellin, D. and Raizen, M. G. Measurement of the Instantaneous Velocity of a Brownian Particle. *Science* **328**, 1673 (2010)
- 10 Gieseler, J., Quidant, R., Dellago, C. and Novotny, L. Dynamic relaxation of a levitated nanoparticle from a non-equilibrium steady state. *Nature Nano.* **9**, 358 (2014)
- 11 Millen, J., Deesuwana, T., Barker, P. F. and Anders, J. Nanoscale temperature measurements using non-equilibrium Brownian dynamics of a levitated nanosphere. *Nature Nano.* **9**, 425 (2014)
- 12 Teufel, J. D. *et al.* Sideband cooling of micromechanical motion to the quantum ground state. *Nature* **475**, 359 (2011)
- 13 Chan, J. *et al.* Laser cooling of a nanomechanical oscillator into its quantum ground state. *Nature* **478**, 89 (2011)
- 14 Bochmann, J., Vainsencher, A., Awschalom, D. D. and Cleland, A. N. Nanomechanical coupling between microwave and optical photons. *Nature Phys.* **9**, 712 (2013)
- 15 Andrews, R. W. *et al.* Bidirectional and efficient conversion between microwave and optical light. *Nature Phys.* **10**, 321 (2014)
- 16 Silanpää, M. A. and Hakonen, P. Optomechanics: Hardware for a quantum network. *Nature* **507**, 45 (2014)
- 17 Safavi-Naeini, A. H. *et al.* Squeezed light from a silicon micromechanical resonator. *Nature* **500**, 185 (2013)
- 18 Chang, D. E. *et al.* Cavity opto-mechanics using an optically levitated nanosphere. *Proc. Natl Acad. Sci. USA* **107**, 1005 (2010)
- 19 Li, T, Kheifets, S. and Raizen, M. G. Millikelvin cooling of an optically trapped microsphere in vacuum. *Nature Phys.* **7**, 527 (2011)
- 20 Gieseler, J., Deutsch, B., Quidant, R. and Novotny, L. Subkelvin Parametric Feedback Cooling of a Laser-Trapped Nanoparticle. *Phys. Rev. Lett.* **109**, 103603 (2012)
- 21 Romero-Isart, O. *et al.*, Large Quantum Superpositions and Interference of Massive Nanometer-Sized Objects. *Phys. Rev. Lett.* **107**, 020405 (2011)
- 22 Horak, P. *et al.* Cavity-induced atom cooling in the strong coupling regime. *Phys. Rev. Lett.* **79**, 4974 (1997)
- 23 Chan, H. W., Black, A. T. and Vuletić, V. Observation of collective-emission-induced cooling of atoms in an optical cavity. *Phys. Rev. Lett.* **90**, 063003 (2003)
- 24 Maunz, P. *et al.* Cavity cooling of a single atom. *Nature* **428**, 51 (2004)
- 25 Leibbrandt, D. R., Labaziewicz, J., Vuletić, V. and Chuang, I. L. Cavity Sideband Cooling of a Single Trapped Ion. *Phys. Rev. Lett.* **103**, 103001 (2009)
- 26 Barker, P. F. and Schneider, M. N. Cavity cooling of an optically trapped nanoparticle. *Phys. Rev. A* **81**, 023826 (2010)
- 27 Romero-Isart, O., Juan, M. L., Quidant, R. and Cirac, J. I. Toward quantum superposition of living organisms. *New J.*

- Phys.* **12**, 033015 (2010)
- <sup>28</sup> Asenbaum, P. *et al.* Cavity cooling of free silicon nanoparticles in high vacuum. *Nature Commun.* **4**, 2743 (2013)
- <sup>29</sup> Kiesel, N. *et al.* Cavity cooling of an optically levitated sub-micron particle. *Proc. Natl Acad. Sci. USA* **110**, 14180 (2013)
- <sup>30</sup> Gieseler, J., Novotny, L. and Quidant, R. Thermal nonlinearities in a nanomechanical oscillator. *Nature Phys.* **9**, 806 (2013)
- <sup>31</sup> Monteiro, T. S. *et al.* Dynamics of levitated nanospheres: towards the strong coupling regime. *New J. Phys.* **15**, 015001 (2013)
- <sup>32</sup> March, R. E., An Introduction to Quadrupole Ion Trap Mass Spectrometry, *J. Mass Spectrom.* **32**, 351 (1997)